From Spectrophotometry to Multispectral Imaging of Ore Minerals in Visible and Near Infrared (VNIR) Microscopy

E Pirard[1], H-J Bernhardt[2], J-C Catalina[3], C Brea[4], F Segundo[5] and R Castroviejo[6]

ABSTRACT

Optical microscopy is a basic but still indispensable tool for examining mineral parageneses in ores. The design and concepts behind the reflected light ore microscope have obviously not been subject to spectacular technical evolutions in the last decades. However, digital imaging capabilities have opened new and stimulating perspectives for automated mineral identification.

Recent works in developing multispectral image analysis (Pirard, 2004) have demonstrated its superior potential with respect to conventional colour imaging, but at the same time reconciliation with spectroscopic databases such as the Quantitative Data File III (Criddle and Stanley, 1993) still needs a more in-depth investigation as well as the possibility to extend both imaging and spectroscopy into the near infrared domain.

In this paper, the authors present results gained from multispectral imaging in the range between 400 and 1000 nm together with spectrophotometric data from the QDFIII database, with an emphasis on minerals that cannot be easily distinguished in the visible spectrum.

INTRODUCTION

Ore microscopy has long been recognised as an essential tool to better understand the genesis of mineral deposits and to help exploration geologists define their targets. However, the visual interpretation of mineral assemblages in terms of geological processes remains a difficult task that requires intensive training and the assimilation of essential textbooks such as the one published by Ramdohr (1980).

In recent years a growing interest for ore microscopy has emerged from the mineral processing community. A new field of investigation has been developing under the attractive name of 'geometallurgy' with the aim of trying to predict as much as possible the behaviour of a given ore within the mineral processing plant on the basis of its mineralogical and microtextural features (Richardson and Williams, 2004). However, efficient prediction of mill performances and precise correlation with metal recovery grades, requires a quantitative approach that traditional/visual ore microscopy cannot provide.

Therefore, a growing demand has been expressed in terms of mineral mapping technologies that could open the way for quantitative mineralogical analysis of ores and at the same time provide insights into the spatial arrangement of the ore constituents.

Though mineral mapping is becoming technically feasible in three-dimensions with the availability of synchrotron based and even desktop X-ray tomography instruments (Ketcham, 2005), it

1. Professeur Ordinaire, Université de Liège, GeMMe, Sart Tilman B52, Liège 4000, Belgium. Email: eric.pirard@ulg.ac.be

2. Professor, Ruhr-Universitaet Bochum, Germany. Email: heinz-juergen.bernhardt@rub.de

3. Head IT Department, AITEMIN, Parque Tecnológico Leganes, Madrid 28919, Spain. Email: jc.catalina@aitemin.es

4. Researcher, Escuela Técnica Superior de Minas, Universidad Politécnica de Madrid, Spain. Email: estrebrea@yahoo.com

5. Researcher, AITEMIN, Parque Tecnológico Leganes, Madrid 28919, Spain. Email: fernando.segundo@aitemin.es

6. Professor, Escuela Técnica Superior de Minas, Universidad Politécnica de Madrid, Spain. Email: ricardo.castroviejo@upm.es
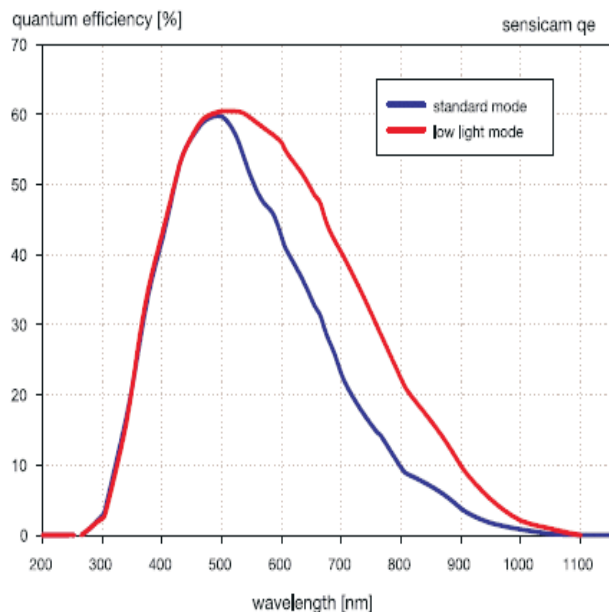
is obvious that for routine observation and for most requirements of textural analysis, two-dimensional imaging is and will remain for the years to come the most reasonable, flexible and productive solution to map minerals in ores.

TWO-DIMENSIONAL IMAGING PRINCIPLES

A digital image is an array of picture elements (pixels) each of them being defined by its unique coordinates and by a set of attributes referring to a property measured locally from the targeted elementary surface.

In a typical grey level image, each pixel has a single attribute:

$$P(x, y) = I_{xy}$$

However, many sensing technologies deliver multiple attributes and hence require the use of a multimodal formalism that can be written as follows:

$$P(x, y) = \left\{ I_{xy}^1, I_{xy}^2, ..., I_{xy}^N \right\}$$

When the different attributes are identical optical properties measured at N different wavelength, the terms multispectral image (typically $3 < N < 20$) or even hyperspectral image ($N > 20$) are preferred (Van der Meer, 2002).

A classical technique to acquire a two-dimensional image is to have a beam (or a sensing device) being swept step by step over a two-dimensional surface. This is basically how a scanning electron microscope (SEM) achieves backscattered electron imaging (BEI) resulting in an image wherein each pixel takes an intensity value proportional to the average atomic number of the targeted mineral:

$$P(x, y) = \overline{Z_{xy}}$$

When using energy dispersive X-ray detectors on the same SEM, the user can generate a multimodal image wherein each image plane refers to the intensity measured for a characteristic ray of a given element:

$$P(x, y) = \left\{ I_{xy}^{Fe}, I_{xy}^S, ..., I_{xy}^{Ni} \right\}$$

An alternative technique to build a two-dimensional image without requiring any sample or sensor movement is to manufacture a miniaturised array containing millions of sensors and place it in the focal plane of a spherical objective. This is only possible at high resolution with a very limited range of sensing technologies among which are the silicon photodiodes used in CCD or CMOS video cameras.

A CCD (or CMOS) video chip delivers a grey level image with values being proportional to the number of photons hitting each cell. The efficiency of this conversion as a function of wavelength should be documented by the manufacturer. A typical efficiency curve is shown in Figure 1.

By using a selection of filters in the optical path it is easy to develop a sequential imaging system for acquiring images at different wavelengths. A so-called true colour image could be obtained in this way by using a set of three 100 nm bandwidth filters corresponding to the triple stimuli of the human eye (red, green and blue). Alternatively, the installation of filters with user defined specifications allows for collecting truly multispectral images across the camera spectral sensitivity range (typically between 350 nm and 1050 nm for Si CCD).

FIG 1 - Quantum efficiency curve for the PCO Sensicam QE camera showing wavelength dependence of the camera response.

REFLECTANCE PROPERTIES OF MINERALS

The reflection of light onto mineral surfaces is a widely documented domain finding many applications in mineral mapping and identification both in remote sensing and close sensing technologies. The diffuse reflection of visible and infrared light by selected mineral species, for example, is documented in a database published by the USGS (Clarke *et al*, 2007). This online database provides spectra of selected minerals between 200 nm and 3000 nm (VNIR – visible and near infrared) with some of the more recent spectra extending into the thermal infrared (TIR) until 16 000 nm.

Such data are essential to interpret measured spectra in terms of possible pure mineral species or mineral assemblages from remote sensing images such as the ones sent by the Advanced Spaceborne Thermal Emission and Reflection Radiometer (ASTER). It also forms the basis of spectral interpretation for instruments such as the HyLogger core scanner (Keeling, Mauger and Huntington, 2004).

With the exception of some major species (pyrite, galena, sphalerite, chalcopyrite, pyrrhotite, ilmenite, etc) (Figure 2), opaque minerals are poorly documented in diffuse reflectance databases because it is difficult to collect pure hand-sized samples and it is exceptional to find occurrences of large sulfide masses in diffuse macroscopic imaging.

Specular reflectance is a special case of diffuse reflectance where the incidence angle is equal and opposite to the reflection angle. The ore microscope has been designed to allow for imaging mineral surfaces at normal incidence provided these are perfectly flat (polished).

The largest compilation of specular reflectance curves for minerals has been published as the Quantitative Data File by Criddle and Stanley (1993). These curves have been limited to the spectral range of visible light (400 - 700 nm) but provide ore microscopists with a complete database of opaque mineral spectra together with microprobe analyses when available. All spectra have been acquired under polarised incident light, allowing the authors to measure the spectral variability (bireflectance) resulting from crystal orientation with respect to the polarisation plane.
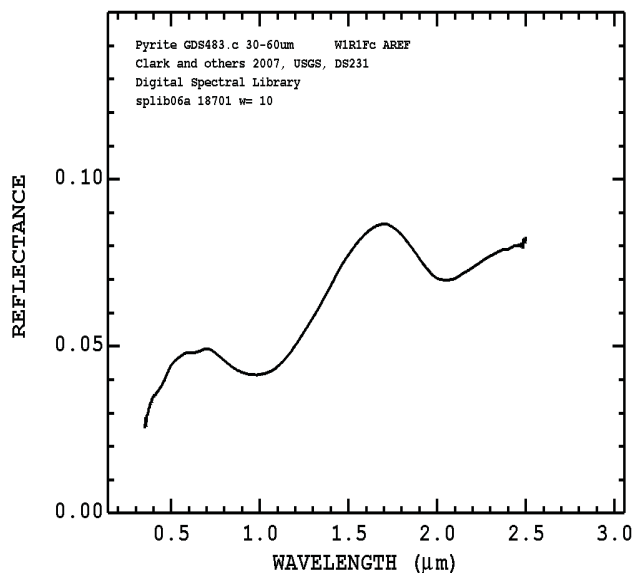

FIG 2 - Diffuse reflectance spectrum of pyrite between 300 nm and 2500 nm as published in the Digital Spectral Library (Clarke *et al*, 2007).

Following Criddle (1998) three major groups of minerals should be distinguished:

- Minerals crystallising in the cubic system have absorption and refraction indices independent of crystal orientation. Hence, their reflectance curves are unique. Important minerals from this group are, among others, pyrite, sphalerite, galena, etc (Figure 3).
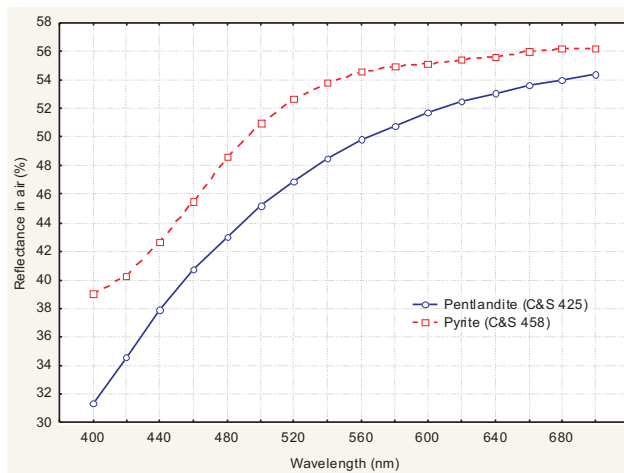

FIG 3 - Specular reflectance spectra of two isotropic minerals pyrite and pentlandite from the Quantitative Data File III (Criddle and Stanley, 1993).

- Minerals belonging to the trigonal, hexagonal or tetragonal systems belong to the family of optically uniaxial crystals. This means that their optical constants have indicatrix corresponding to the axes of crystal symmetry. If a section is cut parallel to the basal plane it will appear isotropic, whereas for any other section reflectance will depend on crystal orientation. Any section will display the ordinary reflectance R_O and a different reflectance indicated by $R_{E'}$. For sections perpendicular to the basal plane, $R_{E'}$ will be maximal and reach the extraordinary reflectance R_E. A typical example is haematite (Pirard, Lebichot and Krier, 2007).

- Finally, all other crystals are optically triaxial and will show a complex bireflectance. The optical literature conventionally designates by R_1 the reflectance curve appearing as minimum at 546 nm and by R_2 the maximum reflectance at this same wavelength (Figure 4).
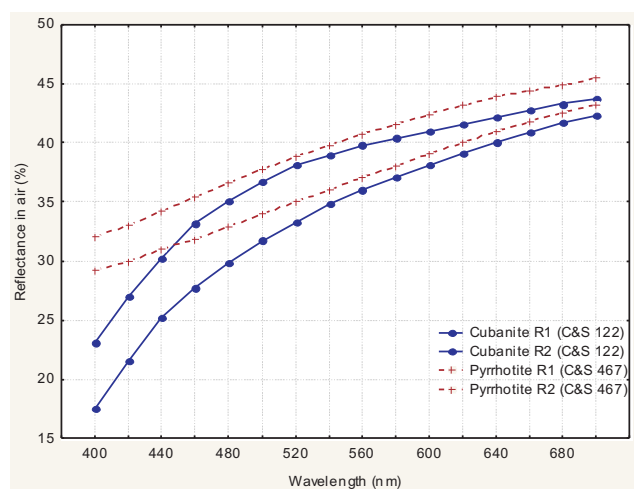

FIG 4 - Specular reflectance spectra of two anisotropic (multiaxial) minerals cubanite and pyrrhotite from the Quantitative Data File III (Criddle and Stanley, 1993).

VISIBLE AND NEAR INFRARED (VNIR) IMAGING IN ORE MICROSCOPY

Instrumentation

The principles of multispectral imaging in ore microscopy have been introduced by Pirard (2004) with particular emphasis on proper image calibration protocols to compensate for unevenness of illumination, optical aberrations and electronic noise.

With the aim of improving imaging capabilities into the near infrared, a multispectral imaging microscope has been developed at AITEMIN based on a Zeiss Axioskop 2 MOT original instrument. The standard hot filter fitted onto the lamp housing to cut any light emission above 700 nm has been removed and replaced by a hybrid hot mirror allowing light up to 1200 nm to pass through.

The illumination tube has been equipped with a rotating filter wheel DTA RPF16 positioned before the field diaphragm. This motorised system allows for the installation of a maximum of 16 filters with a 25 mm diameter. A selection of Melles-Griot filters with 40 nm bandwidth at half maximum (FWHM) have been installed in the filter wheel in order to cover the full spectral range between 400 nm and 1000 nm by steps of 50 nm. Additionally the original C-mount adapter of the trinocular tube with 0.63× magnification has been removed because it induced poor transmission in the near infrared. A lens-less 1× C-mount adapter has been used instead.

The objectives used in the present study were Zeiss Epiplan-Neofluar 5×, 10× and 20× showing good transmittance performance throughout the desired spectral range (Figure 5).

The CCD camera mounted onto the microscope was a Basler Scout with IEEE-1394 connection. It offers a resolution of 1392 × 1040 pixels, programmable integration timing and a signal to noise ratio allowing 12 bit depth imaging if required.

The main differences with respect to the Olympus BX60 system developed at the University of Liège (ULg) are that in the latter case the filter wheel is installed horizontally just in front of
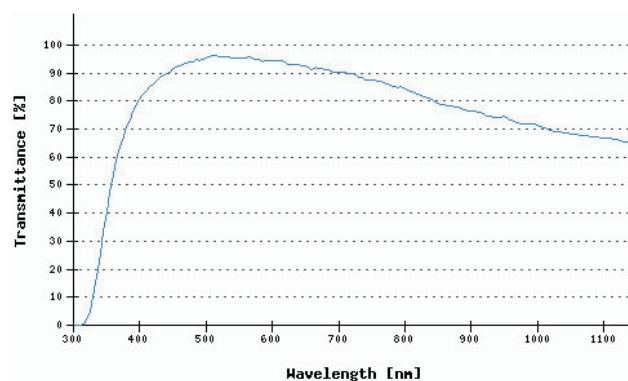

FIG 5 - Transmittance curve of Zeiss EpiPlan Neofluar 10× objective.

the video camera. Moreover, the ULg system uses a selection of 10 nm FWHM interference filters manufactured by Coherent and works with full removal of the hot filter while caring for heat dissipation and limited exposure of the microscope to heat radiation.

Both systems are calibrated using a specular reflectance standard provided commercially by Ocean Optics (STAN-SSH). The reflectance curve obtained from the manufacturer is shown in Figure 6. The reflectance is typically around 89 per cent, although it drops slightly under 85 per cent at 800 nm.
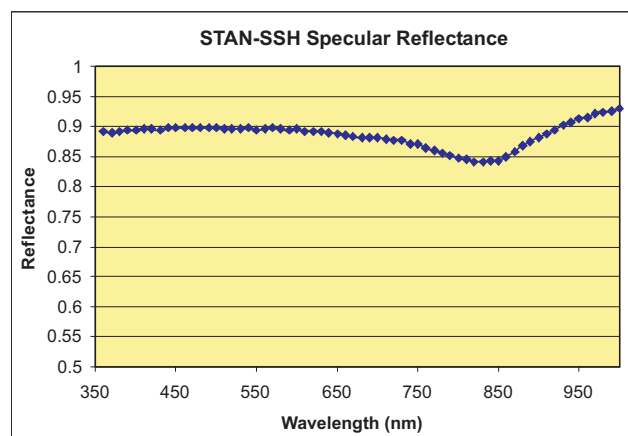

FIG 6 - Specular reflectance spectrum of the Ocean Optics SSH standard used for image calibration.

Image acquisition

Proper multispectral imaging involves a series of steps that can be summarised as follows and are fully automated into the software developed independently in Liège ($Q\mu^2$) and in Madrid (TomaPatron):

- *Integration timing profile* – the integration timing corresponding to each filter are set in such a way that the average grey level output reproduces the specular reflectance curve of Figure 6. By doing so, the conversion of grey level into absolute reflectance values will be straightforward from any image data. The integration timing profile depends solely upon the camera model and the lamp emission spectrum. Hence, these values can be memorised once for all when working with the same camera and a constant lamp voltage.

- *Chromatic aberration* – depending upon the quality of the chromatic correction of the objective the focusing distance can vary significantly with wavelength. Hence focusing

distances are memorised for each wavelength and each objective to ensure optimal focusing. This solution is more reliable than auto-focusing, which is very much dependent upon the content of the scene and can lead to spurious results in case of very uniform surfaces.

- *Background correction* – the images of the high reflectance standard SSH are memorised for each filter versus objective combination. These images will allow for real-time background corrections of all incoming images. Again there is no reason to repeat this procedure if the same microscope operation mode (camera-filter-objective-lamp) has already been used previously. But in order to avoid troubles induced by any modification in the optical path (rotated camera, decentred lamp, lamp ageing, etc) it is advisable to proceed to this standard acquisition regularly.

Once the acquisition conditions are fully determined, the multispectral image acquisition can proceed automatically by acquiring sets of images for each selected scene in the image. For the sake of automatic acquisition of representative sets of images over a whole sample, the $Q\mu^2$ software also includes an option to program the desired surface sampling rate and a focus inference tool to compensate for any slant of the polished surface.

Multispectral images can be analysed interactively to retrieve the spectral signature of any region of interest using either commercial remote sensing software (ENVI, PCI, etc) or the MultiSpec v3.1 software (Landgrebe, 2003). These software also offer a wide range of supervised classification algorithms that will allow for modal computations on an image per image basis although dedicated post processing is often required to improve results (Pirard, 2004).

RESULTS

A selection of ore samples displaying occurrences of important ore minerals have been carefully prepared for multispectral imaging. Within each scene, the operator has selected a number of regions of interest considered as representative of a given mineral and reflectance data have been extracted. Results are presented as median spectra obtained from regions of interest totalling 20 000 to 80 000 pixels and are plotted against a published reflectance spectrum coming from the Quantitative Data File III (Criddle and Stanley, 1993) for sake of comparison (Figure 7).

It is important to note that QDFIII spectra were acquired using polarised light and hence contain R_1 and R_2 spectra or R_O and R_E spectra for anisotropic minerals, whereas in the AITEMIN multispectral imaging system the polariser was removed in order to avoid the effects of bireflectance. Although the microscope geometry and in particular the semi-reflecting mirror cube are suspected to induce parasitic polarisation, it appeared from measurements obtained while rotating highly anisotropic crystals (covellite for instance) that the bireflectance was barely noticeable.

Discrimination among major sulfide species in the visible light range has been documented by several authors, even using large bandwidth colour filters (Berrezueta, 2004). But VNIR imaging until 1000 nm clearly contributes to enhanced discrimination among mineral species. A good example of the benefits of using the 700 - 1000 nm extension is given by secondary copper sulfide parageneses containing minerals such as chalcopyrite, pyrrhotite, cubanite, etc. Figure 8 shows the multispectral image set obtained from a scene with coexisting chalcopyrite, cubanite and pyrrhotite, whereas Figure 9 displays the corresponding VNIR spectra of the minerals.
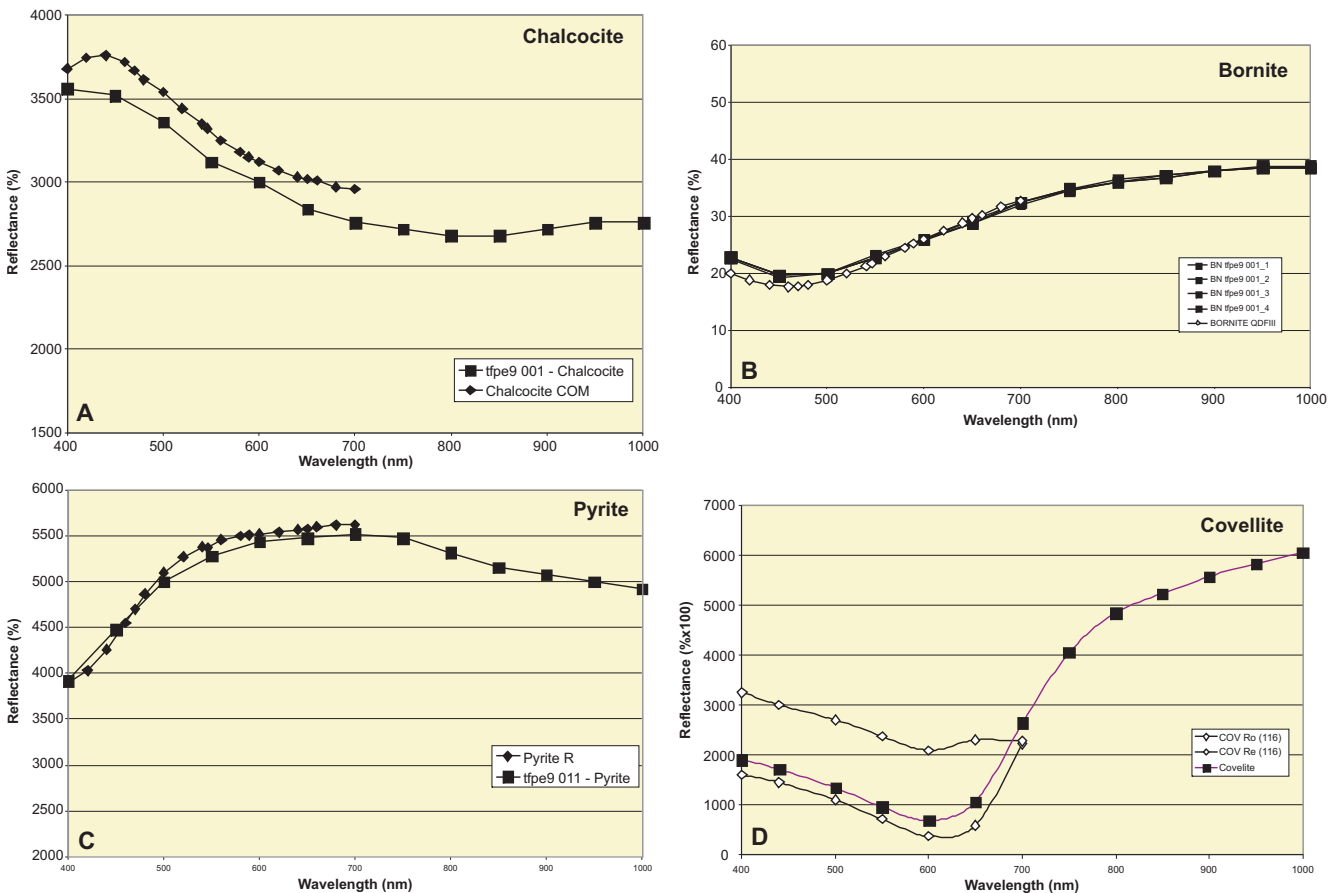

FIG 7 - Specular reflectance curves obtained from spectrophotometry (QDFIII) plotted against extended VNIR reflectance values extracted from the multispectral imaging microscope. (A) Chalcocite, (B) bornite, (C) pyrite, (D) covellite.
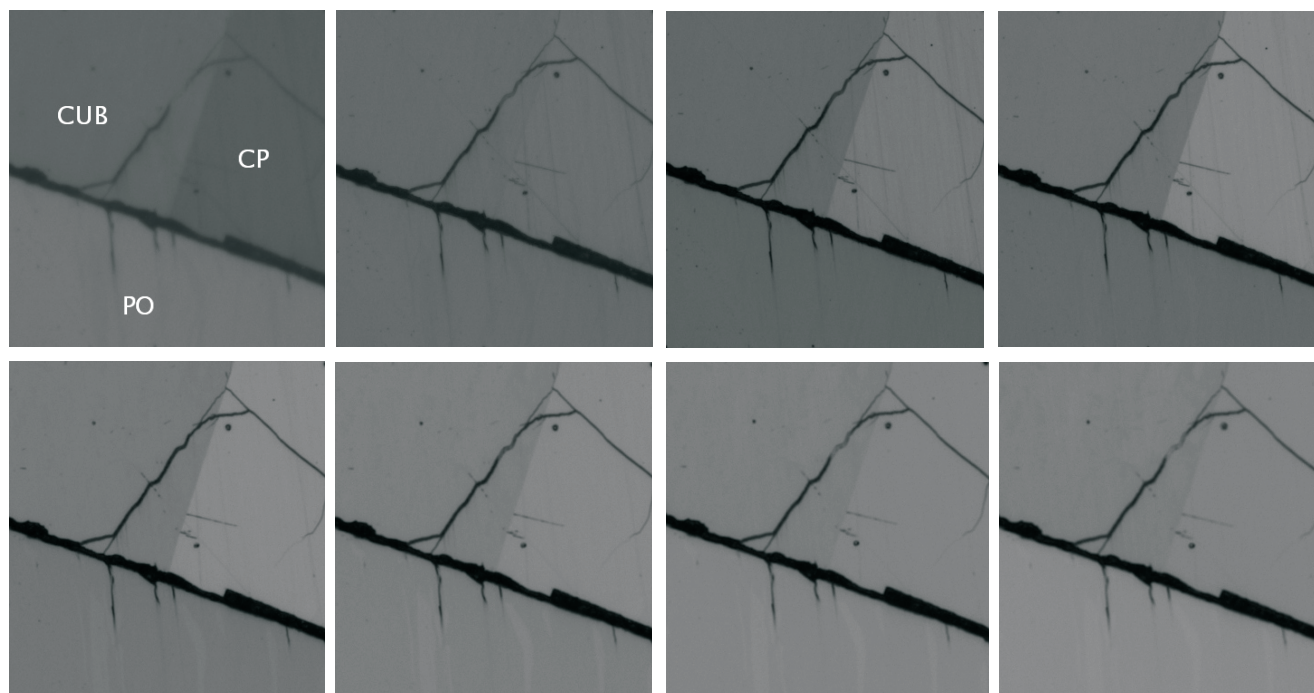
FIG 8 - Images of a region of interest showing intergrown cubanite (CUB), chalcopyrite (CP) and pyrrhotite (PO) at 400 nm, 450 nm, 500 nm, 550 nm, 650 nm, 750 nm, 850 nm and 950 nm.
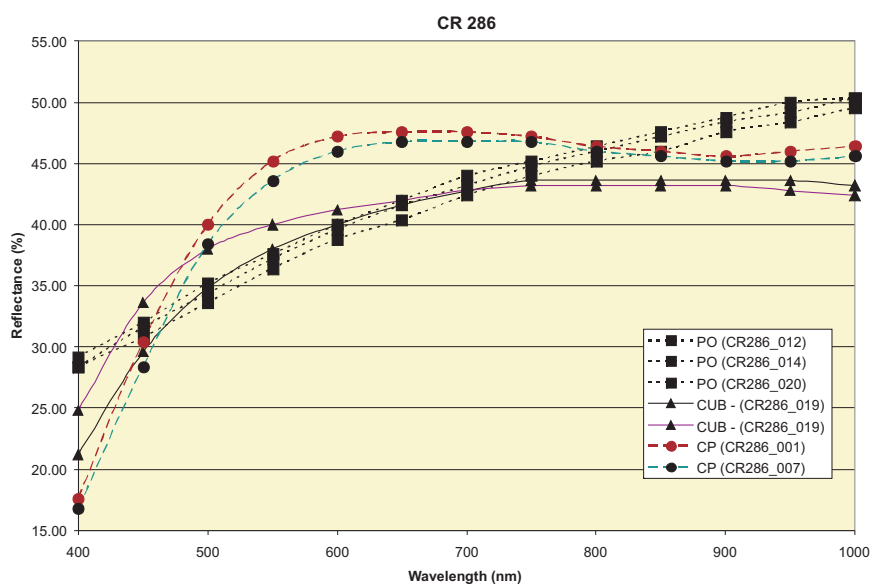

FIG 9 - VNIR spectra computed from images of Figure 8 and corresponding to coexisting chalcopyrite, cubanite and pyrrhotite. Discrimination between chalcopyrite and cubanite/pyrrhotite is optimal around 600 nm, whereas the distinction between cubanite and pyrrhotite appears maximum at 1000 nm.

PERSPECTIVES AND CONCLUSIONS

Preliminary results gained from multispectral imaging of ore minerals between 400 nm and 1000 nm show encouraging results in terms of mineral discrimination potential. The correlation with documented spectrophotometric results is well established and could open the way to an automatic recognition of minerals within multispectral images (unsupervised classification).

However, due to variability of reflectance spectra with mineral composition (especially some minor elements) and with polishing or tarnishing conditions, it is better to think about such a system as a tool for quantification of relative abundances of phases previously pointed by a skilled operator (supervised classification). The major advantages of optical systems are the lower cost of the sensing technology, the flexibility of the operating mode (no vacuum, large sample size, etc) and the speed of operation (a few seconds per image).

This paper demonstrates that using the full potential of a standard silicon sensor and a conventional optical microscope only requires slight changes to the standard technology.

However, the standard design of the optical microscope and especially the precise plane polarisation of the incident light beam will require some additional changes in order for a multispectral imaging system to make full use of additional optical properties such as bireflectance and optical anisotropy.

REFERENCES

Berrezueta, E, 2004. Caracterización de menas mediante análisis digital de imagen, PhD thesis, UPM-ETSI Minas, Madrid.

Clark, R, Swayze, G, Wise, R, Livo, E, Hoefen, T, Kokaly, R and Sutley, S, 2007. USGS digital spectral library splib06a, US Geological Survey, Digital Data Series 231.

Criddle, A J, 1998. Ore microscopy and photometry (1890 - 1998), in *Modern Approaches to Ore and Environmental Mineralogy*, *Short Course Series, 27* (eds: L J Cabri and D J Vaughan) (Mineralogical Association of Canada: Ottawa).

Criddle, A J and Stanley, C J, 1993, *Quantitative Data File for Ore Minerals,* third edition, 635 p (Chapman and Hall: London).

Keeling, J, Mauger, A and Huntington, J, 2004. Spectral core logger update – Preliminary results from the Barns gold prospect, *MESA Journal*, 32:32-36.

Ketcham, R, 2005. Computational methods for quantitative analysis of three-dimensional features in geological specimens, *Geosphere*, 1:32-41.

Landgrebe, D, 2003. *Signal Theory Methods in Multispectral Remote Sensing*, 507 p (John Wiley and Sons).

Pirard, E, 2004. Multispectral imaging of ore minerals in optical microscopy, *Mineralogical Magazine*, 68(2):323-333.

Pirard, E, Lebichot, S and Krier, W, 2007. Particle texture analysis using polarized light imaging and grey level intercepts, *International Journal of Mineral Processing*, 84:299-309.

Ramdohr, P, 1980. The ore minerals and their intergrowths, *Pergamon*, vol 2, 1205 p.

Richardson, J and Williams, S, 2004. Geometallurgical mapping – A new tool for technical risk reduction, in *Proceedings 36th Annual Meeting of Canadian Institute of Mining, Metallurgy and Petroleum*.

Van der Meer, F, 2002. Imaging spectrometry for geological applications, in *Encyclopedia of Analytical Chemistry: Applications, Theory and Instrumentation* (ed: R Meyers), p 14 (Wiley).